

Document downloaded from:

<http://hdl.handle.net/10251/112783>

This paper must be cited as:

Jato-Espino, D.; Sillanpää, N.; Andrés Doménech, I.; Rodríguez-Hernández, J. (2018). Flood Risk Assessment in Urban Catchments Using Multiple Regression Analysis. *Journal of Water Resources Planning and Management*. 144(2):04017085-1-04017085-11. doi:10.1061/(ASCE)WR.1943-5452.0000874



The final publication is available at

[http://doi.org/10.1061/\(ASCE\)WR.1943-5452.0000874](http://doi.org/10.1061/(ASCE)WR.1943-5452.0000874)

Copyright American Society of Civil Engineers

Additional Information

1 Post-print version of 'Jato-Espino, D., Sillanpää, N., Andrés-Doménech, I.,
2 Rodriguez-Hernandez, J. (2018). "Flood Risk Assessment in Urban Catchments
3 Using Multiple Regression Analysis". **J. Water Resour. Plann. Manage.**,
4 144(2): 04017085. DOI: 10.1061/(ASCE)WR.1943-5452.0000874'.
5

6 **Flood risk assessment in urban catchments using multiple** 7 **regression analysis**

8
9 **Daniel Jato-Espino¹; Nora Sillanpää²; Ignacio Andrés-Doménech³; Jorge Rodriguez-**
10 **Hernandez⁴**

11 **Abstract**

12
13
14 Flood assessment in urban catchments is usually addressed through the combination of
15 Geographic Information Systems (GIS) and stormwater models. However, the coupled use of
16 these tools involves a level of detail in terms of hydrological modelling which can be beyond

¹ Postdoctoral Researcher, GITECO Research Group, Universidad de Cantabria, Av. de los Castros 44,
39005, Santander, Spain (corresponding author). E-mail: jatod@unican.es

² Postdoctoral Researcher, Department of Built Environment, Aalto University School of Engineering,
P.O. Box 15200, 00076 Aalto, Finland. E-mail: nora.sillanpaa@aalto.fi

³ Associate Professor, Instituto Universitario de Investigación de Ingeniería del Agua y del Medio
Ambiente (IIAMA), Universitat Politècnica de València, Cno. de Vera s/n, 46022 Valencia, Spain. E-mail:
igando@hma.upv.es

⁴ Associate Professor, GITECO Research Group, Universidad de Cantabria, Av. de los Castros 44,
39005, Santander, Spain (corresponding author). E-mail: rodrighj@unican.es

17 the scope of overall flood management planning strategies. This research consists of the
18 development of a methodology based on Multiple Regression Analysis (MRA) to assess flood
19 risk in urban catchments according to their morphologic characteristics and the geometrical
20 and topological arrangement of the drainage networks into which they flow. Stormwater
21 models were replaced by a combination of Multiple Linear Regression (MLR), Multiple Non-
22 Linear Regression (MNLR) and Multiple Binary Logistic Regression (MBLR), which enabled
23 identifying influential parameters in the maximum runoff rates generated in urban catchments,
24 modelling the magnitude of peak flows across them and estimating flood risk in the nodes of
25 sewer networks, respectively. The results obtained through a real urban catchment located in
26 Espoo (Finland), demonstrated the usefulness of the proposed methodology to provide an
27 accurate replication of flood occurrence in urban catchments due to intense storm events
28 favored by Climate Change, information that can be used to plan and design preventive
29 drainage strategies.

31 **Keywords**

32
33 Flood Risk Management; Geographic Information System; Multiple Regression Analysis;
34 Urban Hydrology

36 **Introduction**

37
38 The interactive effects of urbanization and Climate Change are one of the most important
39 challenges with which human beings will have to deal as a collective in the future ([Hoornweg
40 et al. 2011](#)). Their combination inflicts a particularly forceful impact on stormwater drainage
41 in urban catchments. Growing urbanization contributes to increasing runoff volume and

42 accelerating the time until peak flow occurs, whilst Climate Change is expected to result in an
43 intensification of the hydrological cycle, which might lead to more violent rainfall events
44 ([Huntington 2006](#)). In the end, this might result in localized floods along the sewer networks
45 used to drain urban catchments, which are incapable of conveying such large amounts of water.

46 Urban floods have important consequences in physical, economic, environmental and
47 social terms ([Tingsanchali 2012](#)). These effects have traditionally been divided into tangible
48 and intangible, depending on whether they can be monetized or not ([Smith and Ward 1998](#)).
49 Examples of the former include damage to property or loss of profits, whilst the latter stand for
50 aspects like loss of life or negative impacts on the well-being and environment. The potential
51 impacts of urban floods can also be classified into direct and indirect, according to their
52 spatiotemporal scale. Hence, direct damage is related to any loss caused by the immediate
53 interaction of floods with human beings, properties and the environment, whilst indirect effects
54 concern those which are beyond the limits of the flooded area ([Hammond et al. 2015](#)). All these
55 potential consequences are expected to become more severe and frequent due to the
56 combination of Climate Change with high density of population and large impervious areas
57 ([Huong and Pathirana 2013](#)).

58 However, despite the increasingly important threat posed by this phenomenon, flood
59 management keeps being usually addressed in literature through stormwater models, which are
60 often used in combination with Geographic Information Systems (GIS). [Knebl et al. \(2005\)](#)
61 integrated them in a study to highlight the importance of the degree of imperviousness in urban
62 catchments, which resulted in a decrease in infiltration capacity of the terrain and increased
63 flood risk. [Barco et al. \(2008\)](#) coupled both components to prove that imperviousness and
64 depression storage were the most influential factors in the generation of flow rates in a large
65 urban catchment located in Southern California. [Dongquan et al. \(2009\)](#) combined stormwater
66 models with GIS based on elevation-related data such as flow direction, raster-vector

67 conversion or catchment division to automate the process of rainfall-runoff modelling. Guan
68 et al. (2015) merged both tools to determine the increase in peak flow and runoff volume caused
69 by urbanization in a catchment located in Espoo (Finland) and proposed different alternative
70 drainage techniques to mitigate these effects. Eshtawi et al. (2016) coupled three existing
71 models (SWAT, MODFLOW and MT3DMS) to quantify surface-groundwater interactions in
72 increasingly developed areas, demonstrating the strength of using integrated hydrologic models
73 in the sustainable urban water planning process. Jato-Espino et al. (2016a) presented a GIS-
74 based stormwater modelling approach that demonstrated the potential of permeable pavements
75 and green roofs to attenuate floods in urban catchments in comparison with conventional sewer
76 networks. Beck et al. (2017) described a semi-distributed approach to estimate runoff
77 reductions (TELR) to inform stormwater management decisions, including a series of
78 algorithms for rainfall-runoff transformation and routing and specifications to implement Best
79 Management Practices (BMPs). Hanington et al. (2017) developed and calibrated a fine-scaled
80 quasi-2D hydro-dynamic model (IWRM-LXQ) for interprovincial water resource planning and
81 management, arguing that their approach was especially suitable for assessing hydraulically
82 complex systems at a provincial or district level.

83 The use of tools as those mentioned above is complex and entails a substantial time
84 investment, aspects which are in conflict with the simplicity and promptness required by
85 administrative and public entities to design flood management planning strategies (Ashley et
86 al. 2007). Stormwater models are especially demanding in terms of characterization and
87 simulation to be used by general public or non-modelling planners (Elliott and Trowsdale
88 2007), since they involve making decisions related to infiltration and routing processes and
89 calibrating the parameters that influence the transformation of rainfall to runoff. In contrast,
90 the GIS-related tasks required for creating the input data into these models to run stormwater
91 simulations, which mainly concern catchment delineation and the determination of

92 subcatchment imperviousness and average slope, are easy to compute using basic editing and
93 statistical tools ([Jato-Espino et al. 2016a](#)). Furthermore, GIS are widely implemented systems
94 for multiple purposes related to the management of all kinds of spatial data, so that using them
95 for flood management does not involve an innovation with respect to common resources and
96 practices.

97 As a result of these considerations, the objective of this research was to develop a
98 methodology for flood risk assessment omitting the use of stormwater models. This was
99 achieved through the integration of Multiple Linear Regression (MLR), Multiple Non-Linear
100 Regression (MNLR) and Multiple Binary Logistic Regression (MBLR), which were combined
101 to play the role of stormwater models in a simpler manner. The integrated application of
102 different types of Multiple Regression Analysis (MRA) provided a cutting-edge approach to
103 replicate peak flow rates and predict flooding probabilities in sewer-catchments and opens new
104 lines of research and in the field of urban water planning and management. The usefulness of
105 the proposed methodology was evaluated through a case study of an urban catchment located
106 in Espoo (Finland), which provided the precipitation and flow data required to validate the
107 results at the nodes forming its sewer network.

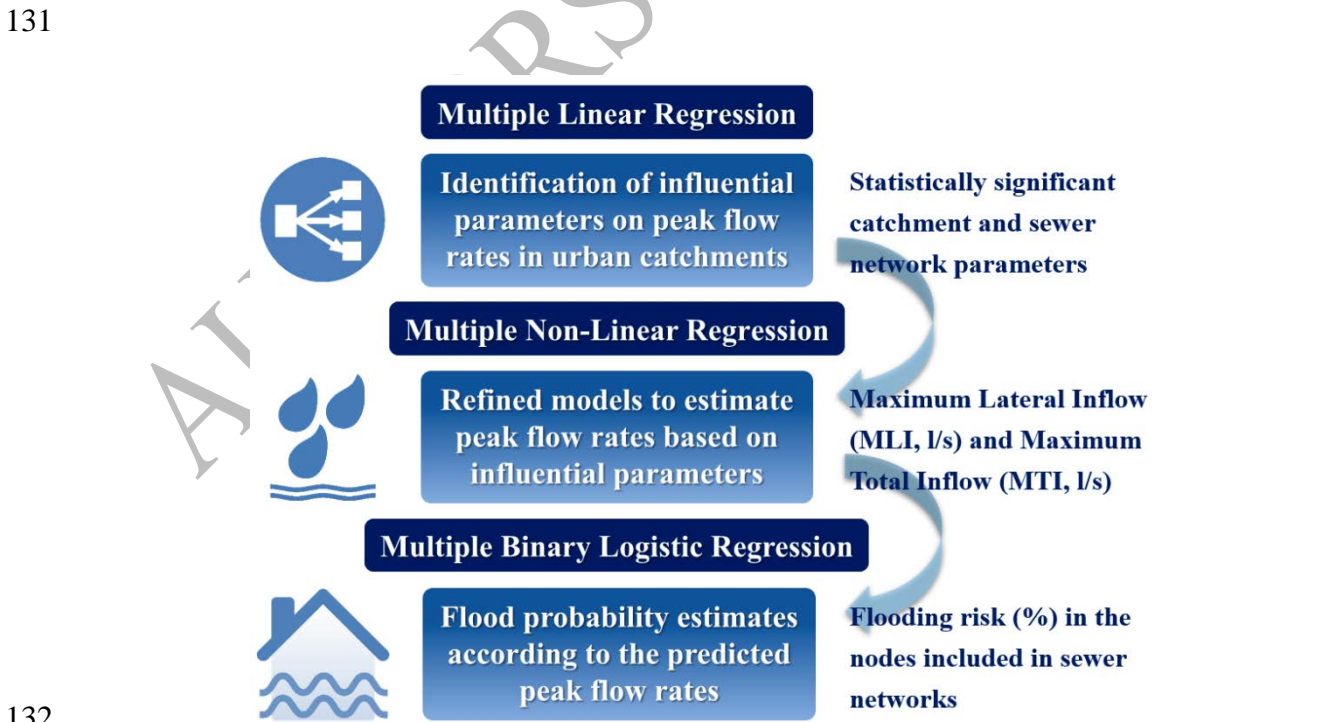
108

109 **Methodology**

110

111 Since the delineation of urban catchments using Geographic Information Systems (GIS) is a
112 widely studied topic in literature ([Knebl et al. 2005](#); [Guan et al. 2015](#); [Jato-Espino et al. 2016a](#)),
113 the methodology proposed in this research only focused on reproducing the role of stormwater
114 models using Multiple Regression Analysis (MRA). The general purpose of MRA is to predict
115 the value of a dependent variable or predictand based on the values of a series of independent
116 explanatory variables or predictors.

117 In the context of this research, Multiple Linear Regression (MLR) was used as an
 118 exploratory analysis to identify relevant parameters to the occurrence of peak flow rates. Next,
 119 the identified parameters were incorporated into a Multiple Non-Linear Regression (MNLR)
 120 framework, in order to boost the prediction accuracy of the magnitude of runoff that might be
 121 generated in urban catchments and conveyed by sewer networks as a result of severe rainfall
 122 events. The magnitude of runoff was presented through the values of Maximum Lateral Inflow
 123 (MLI, l/s) and Maximum Total Inflow (MTI, l/s) produced in urban catchments. The former
 124 stands for the peak of apportionment of surface runoff from the subcatchment areas to each
 125 node in the sewer network, whilst the latter also includes the contribution from preceding nodes
 126 and conduits. Finally, Multiple Binary Logistic Regression (MBLR) models were created from
 127 the estimates of MLI and MTI to determine the probability of flooding in sewer networks,
 128 facilitating the adoption of measures for preventing urban flood events at strategic sites and
 129 maximizing their positive impact and effectiveness. Fig. 1 provides a graphical scheme of the
 130 proposed approach based on the sequential application of these three types of MRA.



132
 133 **Fig. 1.** Scheme of the proposed methodology based on Multiple Regression Analysis (MRA)

134

135 The development of these analyses stemmed from a set of catchment parameters
136 considered for estimating MLI, whose combination with a list of predictors related to the two
137 main elements forming sewer networks (nodes and conduits) enabled modelling both MTI and
138 flooding probability. Table 1 links these parameters to the visual objects required to represent
139 urban drainage systems: subcatchments, nodes and conduits.

140

141 **Table 1.** Parameters for estimating Flooding (%), Maximum Lateral Inflow (MLI, l/s) and Maximum Total Inflow
142 (MTI, l/s) in urban catchments

Predictand	Sub-predictand	Visual object	ID	Predictor
Flooding (%)	MLI (l/s)	Catchment	$x_{1.1}$	Subcatchment area (ha)
			$x_{1.2}$	Degree of imperviousness in the subcatchment (%)
			$x_{1.3}$	Subcatchment width (m)
			$x_{1.4}$	Average slope in the subcatchment (%)
	MTI (l/s)	Sewer network	$x_{2.1}$	Node invert elevation (m)
			$x_{2.2}$	Preceding length of conduit (m)
			$x_{2.3}$	Cumulative preceding length of conduits (m)
			$x_{2.4}$	Subsequent length of conduit (m)
			$x_{2.5}$	Preceding diameter of conduit (m)
			$x_{2.6}$	Cumulative preceding diameter of conduits (m)
			$x_{2.7}$	Subsequent diameter of conduit (m)
			$x_{2.8}$	Preceding slope of conduit (%)
			$x_{2.9}$	Cumulative preceding slope of conduits (%)
			$x_{2.10}$	Subsequent slope of conduit (%)

143

144 These predictors were selected to result in a set of basic variables easy to acquire and/or
145 compute, in order to facilitate the implementation of the proposed methodology worldwide.
146 Therefore, the length and depth of conduits (pipes) and nodes (manholes), respectively, were
147 the inputs required to parameterize the drainage network in the study area, whilst the
148 subcatchments forming it were characterized according to their area, percentage of
149 imperviousness, slope and width, which was estimated dividing their area by the average length
150 of the flow paths from the furthest drainage points. All these catchment-related variables were
151 determined using GIS-based editing and zonal statistics tools.

152 As pointed out by Yao et al. (2017), who highlighted the complexity of urban hydrology
153 for water resources planning and management, the relationships between rainfall-runoff
154 processes and spatial patterns is a key factor to manage flood risks in small catchments. In fact,
155 the need for designing strategies for flood risk prevention based on proactive spatial planning
156 has been identified as a crucial aspect to ensure the resilience of urban socio-ecological systems
157 (Hegger et al. 2016).

158

159 **Identification of relevant parameters for peak flow generation**

160

161 The justification of which parameters related to the morphology of urban catchments and the
162 geometry of sewer networks (Table 1) contributed more to explaining the values of MLI and
163 MTI associated with different storm events was carried out using MLR. MLR consists of
164 modelling the relationship between n predictors x_n and a predictand y through a linear
165 expression as formulated in Eq. (1) (Aiken et al. 2003):

166

$$y = b_0 + \sum_{i=1}^n b_i \cdot x_i + \varepsilon \quad (1)$$

167

168 where b_i is the weight that indicates the importance of each predictor in the model. All
169 the information that cannot be provided by the independent variables is completed by b_0 and
170 ε , which are a constant and the residuals, respectively. A significance level of $\alpha = 0.05$ (Fisher
171 1925) was the threshold which determined whether a parameter was statistically significant for
172 estimating MLI and MTI or not.

173

174 Therefore, this first step had the sole purpose of justifying the selection of parameters
that contributed the most to reach high values of MLI and MTI from a physical point of view.

175 The use of MLR was deemed essential to ensure the hydrological and hydraulic validity of the
176 proposed approach, since the clarity of these contributions might be distorted if evaluated
177 through MNLR, due to the increased complexity involved by the inclusion of non-linear terms.
178 This course of action was adopted based on the results of similar previous studies ([Jato-Espino
179 et al. 2017](#)), which applied MNLR to refine the prediction accuracy of relevant parameters
180 identifiable using MLR.

181

182 **Modelling of Maximum Lateral Inflow and Maximum Total Inflow**

183

184 Once the identification of catchment and sewer network parameters proving to be statistically
185 significant for the generation of peak flow rates was accomplished, MNLR was used to
186 combine them in the creation of non-linear equations for predicting both MLI and MTI with
187 high accuracy. Unlike Eq. (1), the formula associated with MNLR also includes interactions
188 and quadratic terms, as shown in Eq. (2):

189

$$y = b_0 + \sum_{i=1}^n b_i \cdot x_i + \sum_{i=1}^n b_{ii} \cdot x_i \cdot x_i + \sum_{i=1}^n \sum_{j=1}^n b_{ij} \cdot x_i \cdot x_j + \varepsilon \quad (2)$$

190

191 where b_{ii} and b_{ij} are the weights that indicate the importance of the quadratic and
192 interaction terms in the model.

193

194 Since the objective of this paper was the design of a methodology to assess flood risk
195 in urban catchments for water resources planning and management, the predicted R^2 coefficient
196 was chosen to measure the goodness-of-fit of MNLR, in order to validate the proposed
approach for modelling new cases. This coefficient consists of removing each observation from

197 the dataset in the MNLR, predicting the regression equation and calculating how well the model
198 estimates the omitted observation.

199 To further ensure the validity of the MNLR models built, their residuals were analyzed
200 based upon the assumptions of normality, homoscedasticity and independence. The fulfillment
201 of these assumptions was graphically verified using the following residual plots (Osbourne and
202 Waters 2002): normal probability plot (Q-Q plot), standardized residuals vs. standardized
203 predicted values plot and standardized residuals vs. observation order plot.

204 The equations derived from these MNLR were used to estimate the values of MLI and
205 MTI in urban catchments straightforward through a series of predictors as those listed in Table
206 1. Such equations were further processed to incorporate rainfall intensity (I) into them, in order
207 to allow predicting the magnitude of flooding for different precipitation scenarios accordingly.
208 To this end, MLR was used again to determine the constant b_0 and weights b_i , b_{ii} and b_{ij} of the
209 terms in the MNLR models as a function of I through Eq. (3). The estimates obtained using
210 this expression were inputs in the calculation of the flooding probability of the nodes forming
211 urban sewer networks through MBLR.

$$b_0 \vee b_i \vee b_{ii} \vee b_{ij} = b'_0 + b'_1 * I \quad (3)$$

213

214 **Prediction of flooding probability**

215

216 MBLR was used to integrate the knowledge generated through the application of the other
217 types of MRA considered in the methodology (MLR and MNLR) to assess flood risk in urban
218 catchments. MBLR is another variant of MLR characterized by the dichotomous nature of the
219 predictand, which only has two possible outcomes. Hence, MBLR predicts the probability Pr

220 that a certain characteristic is present in the predictand y from the values of the predictors x_i .

221 The analytic expression for a MBLR model based on the logit link function is given in Eq. (4):

222

$$\Pr(y = 1 | x_i) = \frac{\exp(y')}{1 + \exp(y')} = \frac{\exp(b_0 + \sum_{i=1}^n b_i \cdot x_i)}{1 + \exp(b_0 + \sum_{i=1}^n b_i \cdot x_i)} \quad (4)$$

223

224 where $y = 1$ indicates that the characteristic is present in observation i . In this case, the

225 two outcomes for the predictand were “yes” and “no”, depending on whether the nodes of

226 sewer networks were flooded or not after the occurrence of heavy rainfall events, and the

227 predictors were the parameters included in Table 1.

228 In addition to the predictors and the predictand, MBLR enables incorporating another

229 term into the analysis, known as frequency, which is an indicator of the number of times that

230 the characteristic to be modelled is present. This concept was adapted to the purpose of this

231 study to express how susceptible the nodes in sewer networks were to flooding. Hence, based

232 on the parameters considered in the methodology so far, the frequency was defined as the ratio

233 of MTI to MLI. This value was expected to provide a measure of the sensitivity of the nodes

234 of sewer networks to reach their full capacity, since it combines two of the main factors

235 favouring the occurrence of floods: accumulation and immediate contribution.

236 Therefore, flooding was a dichotomous dependent variable (i.e. its presence in a node

237 is either “yes” or “no”) to be estimated using a series of catchment and sewer network

238 continuous independent variables modulated by a frequency term representing the peak flow

239 conditions in the sewer network. Consequently, the application of Eq. (4) yielded a probability

240 indicating how likely a certain node was to be flooded; i.e. the worse the combinations of values

241 in the predictors and the higher ratios of MTI to MLI, the closer the probability (expressed as

242 a decimal) of that node to be 1.

243 The goodness-of-fit evaluation of MBLR slightly differed from that used for MNL, R,
244 due to the particular nature of the predictand in this type of MRA. The quality of MBLR models
245 was assessed through the adjusted deviance R^2 coefficient and the Akaike Information
246 Criterion (AIC) (Akaike 1973), which enabled the comparison of models with different
247 predictors. Furthermore, the Hosmer-Lemeshow test was applied to check whether the
248 deviation between estimated and observed probabilities was unpredictable by the binomial
249 distribution (Hosmer and Lemeshow 2000). This test was found to be more suitable than the
250 Deviance or Pearson tests due to the binary/response/frequency format of the data. The fact
251 that the predictand was a binary outcome made the verification of residuals described for
252 MNL nonsensical.

253 The application and testing of the proposed framework enabled detecting which
254 subcatchments and nodes required priority actions in terms of urban drainage planning and
255 management, based on the values of peak runoff and flooding probability obtained through the
256 subsequent application of Eqs. (2), (3) and (4).

257

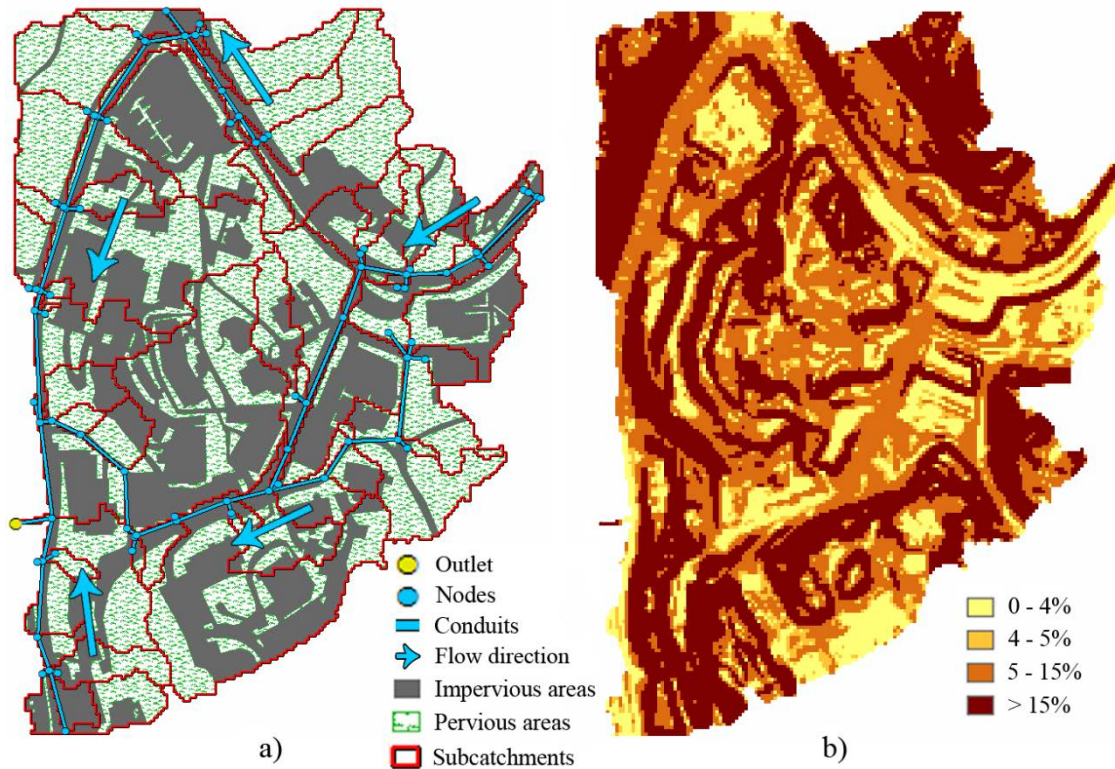
258 **Results and discussion: a case study in Espoo, Finland**

259

260 The proposed methodology was implemented through a case study consisting of an urban
261 catchment located in Espoo, Finland (see (Sillanpää and Koivusalo 2015) for further details).
262 Fig. 2a) shows the spatial arrangement of the sewer network corresponding to this catchment,
263 which was provided by the Helsinki Region Environmental Services Authority HSY and
264 consisted of 75 nodes and 80 conduits, the 79 subcatchments forming the whole catchment
265 area, which covered 10.535 ha, and the relationship between impervious and pervious areas in
266 the catchment, which were delineated from the orthophoto of the study area (Jato-Espino et al.
267 2017). Fig. 2b) depicts the values of slope in the catchment, which were determined and

268 classified from the Digital Terrain Model of the study area using Geographic Information
269 Systems (GIS) tools (Jato-Espino et al. 2016b).

270



272

272 **Fig. 2.** a) Sewer network, subcatchments and impervious and pervious areas in the study catchment b) Slope (%)
273 in the study catchment

274

275 The rainfall events used in this paper were taken from Jato-Espino et al. (2017), who
276 modelled the study catchment in SWMM 5.1.010 (USEPA 2016) using three calibration (CAL
277 1, CAL 2 and CAL 3) and validation (VAL 1, VAL 2 and VAL 3) rainfall events (Table 2).
278 These simulations reproduced the real hydrographs monitored at the outlet of the catchment
279 with high accuracy, as demonstrated by the goodness-of-fit measures used to test them: Root-
280 Sum Squared Error (RSSE), coefficient of determination (R^2) and Nash–Sutcliffe model
281 efficiency coefficient (E) (Table 2).

282 The study catchment was re-simulated with the calibrated parameters for different
283 return periods and Climate Change scenarios: RCP4.5 and RCP8.5 (Moss et al. 2008). Table 2

284 lists the values of duration, depth and intensity associated with four combinations of Climate
 285 Change scenario and return period (T) producing floods of different magnitude in the
 286 catchment, which were determined through its lag time and the coupling of Intensity–Duration–
 287 Frequency (IDF) curves and the Alternating Block Method, respectively.

288

289 **Table 2.** Summary of the rainfall events used to test the proposed methodology. Adapted from Jato-Espino et al.
 290 (2017)

Event	Duration (min)	Rainfall depth (mm)	Intensity (mm/h)	RSSE	R ²	E
CAL 1	352	5.0	0.85	81.94	0.91	0.85
CAL 2	686	37.4	3.27	212.81	0.93	0.86
CAL 3	418	12.2	1.75	92.67	0.96	0.93
VAL 1	396	5.2	0.79	42.46	0.97	0.97
VAL 2	288	9.0	1.88	68.26	0.95	0.92
VAL 3	408	23.4	3.44	115.64	0.97	0.96
RCP4.5; T = 5 yr.	106	19.0	10.75	-	-	-
RCP8.5; T = 5 yr.	106	25.6	14.48	-	-	-
RCP4.5; T = 50 yr.	106	31.5	17.84	-	-	-
RCP8.5; T = 25 yr.	106	38.0	21.51	-	-	-

291

292 **Identification of relevant parameters for peak flow generation in the study** 293 **catchment**

294

295 Multiple Linear Regression (MLR) enabled identifying which predictors listed in Table 1 were
 296 statistically significant for the generation of peak flow rates and, by extension, determining
 297 their degree of contribution to producing high values of Maximum Lateral Inflow (MLI) and
 298 Maximum Total Inflow (MTI). MLR models were built stepwise in Minitab 17 (Minitab Inc
 299 2016) to select only those predictors that were statistically significant to explain variations in
 300 MLI and MTI at the 95% confidence level (p-value < 0.05).

301 The results obtained for the modelling of MLI revealed that three parameters were
 302 statistically significant for estimating this predictand (p-value < 0.05): $x_{1,1}$ (Subcatchment
 303 area), $x_{1,2}$ (Degree of imperviousness in the subcatchment) and $x_{1,4}$ (Average slope in the

304 subcatchment). The most influential predictor for estimating MLI was found to be $x_{1.1}$ with an
305 average contribution of 82.52%, followed by $x_{1.2}$ and $x_{1.4}$ with 6.03% and 2.04%, respectively.
306 Although their weights were different depending on the characteristic of the rainfall events
307 used (Table 2), the contribution of the predictors considered was very similar in all cases. This
308 homogeneity of values under different rainfall events validates the results achieved, since it
309 indicates that the impacts of $x_{1.1}$, $x_{1.2}$ and $x_{1.4}$ on MLI were very similar both when considering
310 common (CAL 1, CAL 2, CAL 3, VAL 1, VAL 2 and VAL 3) and extreme storms.
311 Furthermore, the relationships between these predictors and MLI were logical, because larger
312 subcatchments provide more opportunities to accumulate runoff and both impervious and steep
313 areas facilitate the rapid conveyance of water. Hence, areas devoid of divisions due to drainage
314 network deficiencies, built-up surfaces and topographically problematic sites were found to be
315 more prone to produce high lateral inflows in urban catchments. Consequently, the mitigation
316 of excessive runoff should be approached merging both nature and artificial solutions aimed at
317 vegetating urban surfaces and also ensuring drainage support services, respectively.

318 Since the methodology was a stepped process in which the values of MTI in the nodes
319 were partially calculated from those of MLI, the latter was included in the MLR models for
320 estimating the former as a single predictor, in addition to those related to the sewer network
321 (Table 1). As a result, x_1 (MLI) emerged as one of the two parameters proving to be statistically
322 significant for predicting MTI, along with $x_{2.3}$ (Cumulative preceding length of conduits). In
323 this case, $x_{2.3}$ was clearly the most important factor influencing the values of MTI in the nodes
324 of the study catchment, with an average contribution of 97.39%. Again, both predictors were
325 positively correlated to the predictand, since they contributed to increased runoff accumulation
326 throughout the sewer network and the catchment, respectively. In fact, x_1 was statistically
327 significant only for the extreme events. However, since they represented the situations in which
328 floods occurred for different combinations of climate scenario and return period, this parameter

329 was concluded to be relevant for the purpose of this research and was therefore not removed
 330 from further analyses.

331 All these results enabled validating the MLR models built for identifying statistically
 332 significant parameters for estimating peak flow rates and, therefore, using the information
 333 related to their degree of contribution to create MNLR models to predict MLI and MTI with
 334 high accuracy.

335

336 **Modelling of Maximum Lateral Inflow and Maximum Total Inflow in the** 337 **study catchment**

338

339 Multiple Non-Linear Regression (MNLR) was used to fit the values of MLI and MTI obtained
 340 in all the nodes of the study catchment (Fig. 2a) through the simulations run in SWMM (Jato-
 341 Espino et al. 2017) for the rainfall events that produced floods in the study catchment (Table
 342 2), based on the knowledge acquired from the application of MLR to determine which
 343 catchment and sewer network parameters were more relevant for producing peak flow rates.
 344 Table 3 and Table 4 summarize the MNLR models determined for predicting both MLI and
 345 MTI.

346

347 **Table 3.** Summary of the Multiple Non-Linear Regression (MNLR) models built for the estimation of Maximum
 348 Lateral Inflow (MLI, l/s)

Event	Equation	Pred. R^2
RCP4.5; T = 5 yr.	$MLI = (3.21 - 54.85 * x_{1.1} * x_{1.1} + 1.64 * x_{1.1} * x_{1.2} + 1.51 * x_{1.1} * x_{1.4})^{1/0.845}$	0.95
RCP8.5; T = 5 yr.	$MLI = (4.17 - 75.00 * x_{1.1} * x_{1.1} + 2.29 * x_{1.1} * x_{1.2} + 2.04 * x_{1.1} * x_{1.4})^{1/0.845}$	0.96
RCP4.5; T = 50 yr.	$MLI = (4.94 - 93.04 * x_{1.1} * x_{1.1} + 2.90 * x_{1.1} * x_{1.2} + 2.51 * x_{1.1} * x_{1.4})^{1/0.845}$	0.96
RCP8.5; T = 25 yr.	$MLI = (5.77 - 113.55 * x_{1.1} * x_{1.1} + 3.60 * x_{1.1} * x_{1.2} + 3.02 * x_{1.1} * x_{1.4})^{1/0.845}$	0.96

349

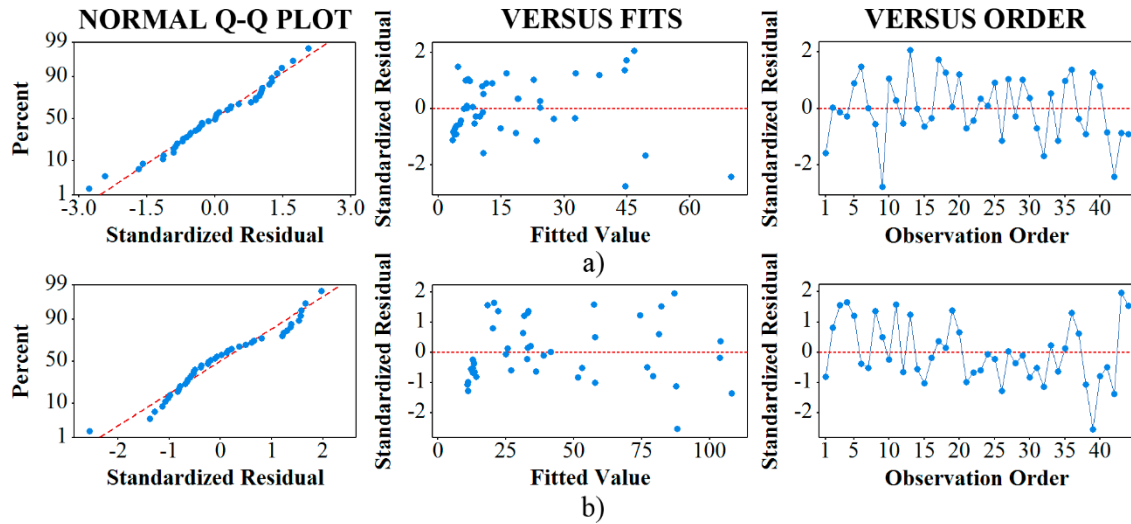
350 **Table 4.** Summary of the Multiple Non-Linear Regression (MNL) models built for the estimation of Maximum
 351 Total Inflow (MTI, l/s)

Event	Equation	Pred. R^2
RCP4.5; T = 5 yr.	$MTI = (6.03 + 9.50 * 10^{-2} * x_{2,3} + 6.39 * 10^{-2} * x_1 - 2.50 * 10^{-5} * x_{2,3} * x_{2,3})^{1/0.682}$	0.96
RCP8.5; T = 5 yr.	$MTI = (7.70 + 1.15 * 10^{-1} * x_{2,3} + 7.11 * 10^{-2} * x_1 - 4.00 * 10^{-5} * x_{2,3} * x_{2,3})^{1/0.682}$	0.95
RCP4.5; T = 50 yr.	$MTI = (8.98 + 1.30 * 10^{-1} * x_{2,3} + 7.54 * 10^{-2} * x_1 - 5.10 * 10^{-5} * x_{2,3} * x_{2,3})^{1/0.682}$	0.93
RCP8.5; T = 25 yr.	$MTI = (10.04 + 1.42 * 10^{-1} * x_{2,3} + 7.90 * 10^{-2} * x_1 - 6.20 * 10^{-5} * x_{2,3} * x_{2,3})^{1/0.682}$	0.92

352

353 The high values of predicted R^2 reached for both models, which were always above 0.9,
 354 ensured their reliability for making new estimates of MLI and MTI and validated the two-step
 355 approach based on the combination of MLR and MNL. Furthermore, their residuals met the
 356 assumptions on which Multiple Regression Analysis (MRA) is based: normality,
 357 homoscedasticity and independence. For instance, Fig. 3 provide visual verification of the
 358 fulfilment of these assumptions for the worst regression models in Table 3 and Table 4 in terms
 359 of goodness-of-fit: RCP4.5; T = 5 yr. (MLI) and RCP8.5; T = 25 yr. (MTI). The approximate
 360 straight line in the Q-Q plots ensured the normality of residuals, whilst their random and non-
 361 curvilinear distributions around the horizontal axis in the standardized residuals versus fits
 362 plots confirmed the homoscedasticity of the regression models. Finally, the residuals versus
 363 order plots suggested that there was no serial correlation and their independence could also be
 364 assumed.

365



366

367 **Fig. 3.** Residual analyses for the Multiple Non-Linear Regression (MNL) models built for the estimation of a)
 368 Maximum Lateral Inflow (MLI, l/s) for the RCP4.5 scenario and a return period of 5 years and b) Maximum
 369 Total Inflow (MTI, l/s) for the RCP8.5 scenario and a return period of 25 years

370

371 To facilitate the application of the equations for estimating MLI and MTI shown in
 372 Table 3 and Table 4 according to the characteristics of rainfall events, their constant b_0 and
 373 weights b_i , b_{ii} and b_{ij} (Eq. (2)) were fitted using MLR again with the intensity (I) of the Climate
 374 Change storms listed in Table 2 as predictor. Table 5 collects the equations obtained to predict
 375 these weights for both MLI and MTI.

376

377 **Table 5.** Summary of the Multiple Linear Regression (MLR) models built for the estimation of the constant (b_0)
 378 and weights (b_i , b_{ii} and b_{ij}) for the Maximum Lateral Inflow (MLI, l/s) and Maximum Total Inflow (MTI, l/s)

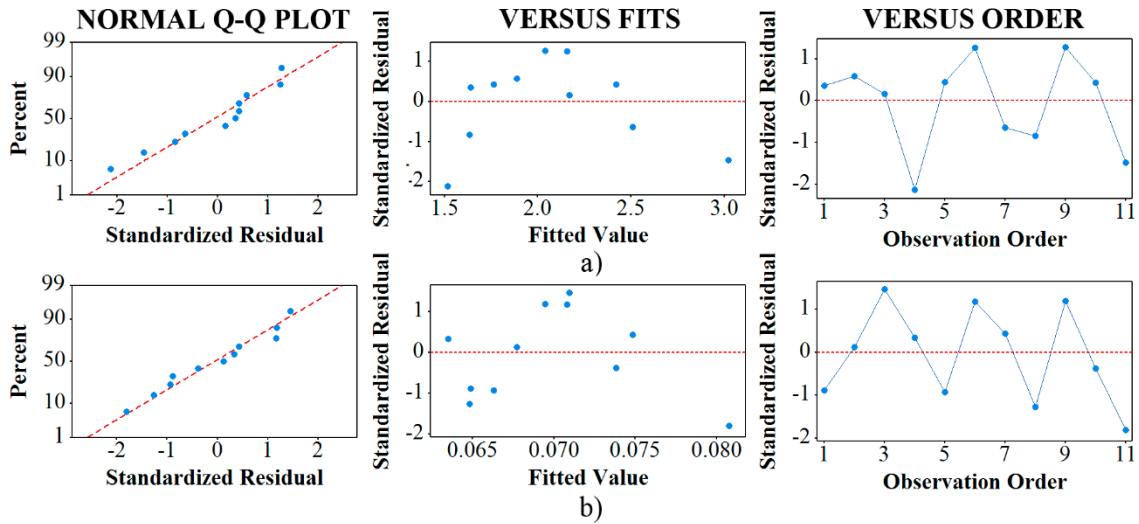
Variable	Equation	Pred. R^2
MLI	$b_{1.0} = 0.692 + 0.238 * I$	1.00
	$b_{1.1*1.1} = 3.675 - 5.434 * I$	1.00
	$b_{1.1*1.2} = -0.329 + 0.182 * I$	1.00
	$b_{1.1*1.4} = 0.008 + 0.140 * I$	1.00
MTI	$b_{2.0} = 2.115 + 0.380 * I$	0.97
	$b_{2.3} = 0.049 + 0.005 * I$	0.96
	$b_1 = 0.046 + 0.002 * I$	0.88
	$b_{2.3*2.3} = 1.111 * 10^{-5} - 3.471 * 10^{-5} * I$	0.98

379

380 Again, the MLR models obtained highlighted by the excellent values of predicted R^2

381 achieved and enabled accepting the assumptions of MRA, as proven in Fig. 4, which depicts

382 the residuals plots associated with the less accurate equations in Table 5: interaction between
 383 catchment area and average slope in the subcatchment ($b_{1.1*1.4}$) and b) Maximum Lateral
 384 Inflow (MLI) (b_1)
 385



386
 387 **Fig. 4.** Residual analyses for the Multiple Linear Regression (MLR) models built for the estimation of weights
 388 for a) interaction between subcatchment area and average slope in the subcatchment ($b_{1.1*1.4}$) and b) Maximum
 389 Lateral Inflow (MLI) (b_1)
 390

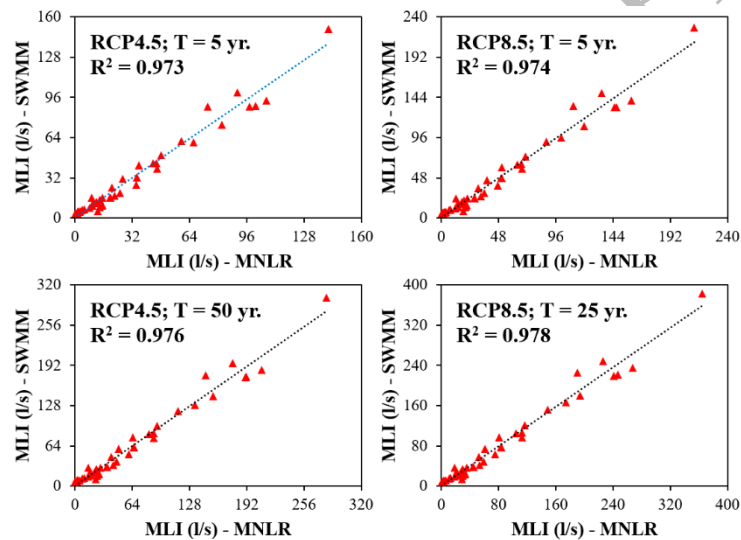
391 The merger of the expressions contained in Table 3 and Table 4 with those determined
 392 in Table 5 yielded Eqs. (5) and (6), whose application allowed calculating the values of MLI
 393 and MTI in the study catchment from the sole use of easy-to-compute GIS-based factors and
 394 the intensity of the rainfall event to be assessed.

$$\begin{aligned}
 MLI = & [(0.692 + 0.238 * I) + (3.675 - 5.434 * I) * x_{1.1} * x_{1.1} + (-0.329 + 0.182 * I) \\
 & * x_{1.1} * x_{1.2} + (0.008 + 0.140) * x_{1.1} * x_{1.3}]^{1/0.845}
 \end{aligned}
 \tag{5}$$

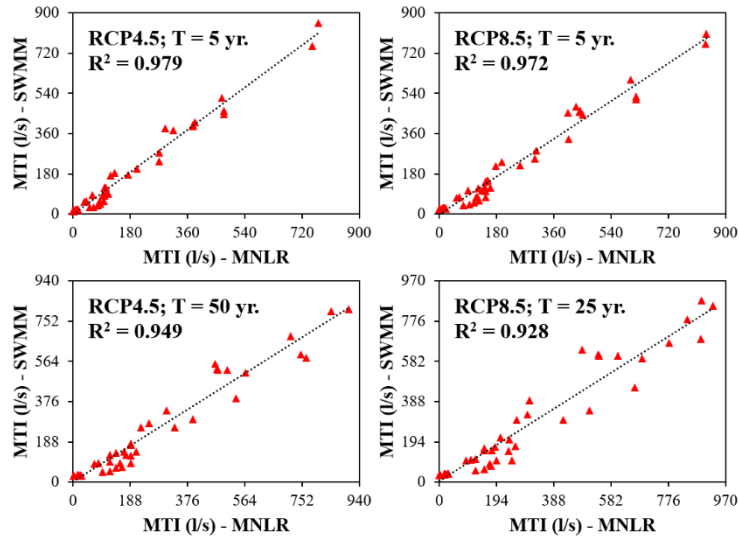
$$\begin{aligned}
 MTI = & [(2.115 + 0.380 * I) + (0.049 - 0.005 * I) * x_{2.1} + (0.046 + 0.002 * I) * x_1 \\
 & + (1.111 * 10^{-5} - 3.471 * 10^{-5} * I) * x_{2.1} * x_{2.1}]^{1/0.682}
 \end{aligned}
 \tag{6}$$

397

398 The particularization of Eqs. (5) and (6) to the Climate Change storm events shown in
399 Table 2 produced the values of MLI and MTI represented in Fig. 5 and Fig. 6, respectively.
400 Their comparison with the results obtained through simulation in SWMM resulted in values of
401 R^2 higher than 0.9 in all cases, demonstrating the accuracy of the proposed framework based
402 on the combination of MLR and MNLR to fit the lateral and total peak flow rates in the nodes
403 of the study area due to a series of storms with different intensities and durations, which in turn
404 enable putting a focus on the elements in urban catchments which most contribute to producing
405 flood events and taking water-related actions accordingly.
406



407
408 **Fig. 5.** Fit between the values of Maximum Lateral Inflow (MLI, l/s) obtained through stormwater simulations
409 and those determined using Multiple Non-Linear Regression (MNLR)
410



411

412

Fig. 6. Fit between the values of Maximum Total Inflow (MTI, l/s) obtained through stormwater simulations and those determined using Multiple Non-Linear Regression (MNLR)

413

414

415 Prediction of flooding probability in the study catchment

416

417 The last step to accomplish the implementation of the proposed methodology to the study
 418 catchment consisted of combining the parameters listed in Table 1 with the values of MLI and
 419 MTI predicted through Eqs. (5) and (6), in order to build Multiple Binary Logistic Regression
 420 (MBLR) models for predicting the probability of flooding throughout the sewer network. The
 421 equations to estimate y' (see Eq. (4)) for the four rainfall scenarios under consideration are
 422 provided in Table 6.

423

424 **Table 6.** Summary of the Multiple Binary Logistic Regression (MBLR) models built for the estimation of
 425 Flooding Probability (%)

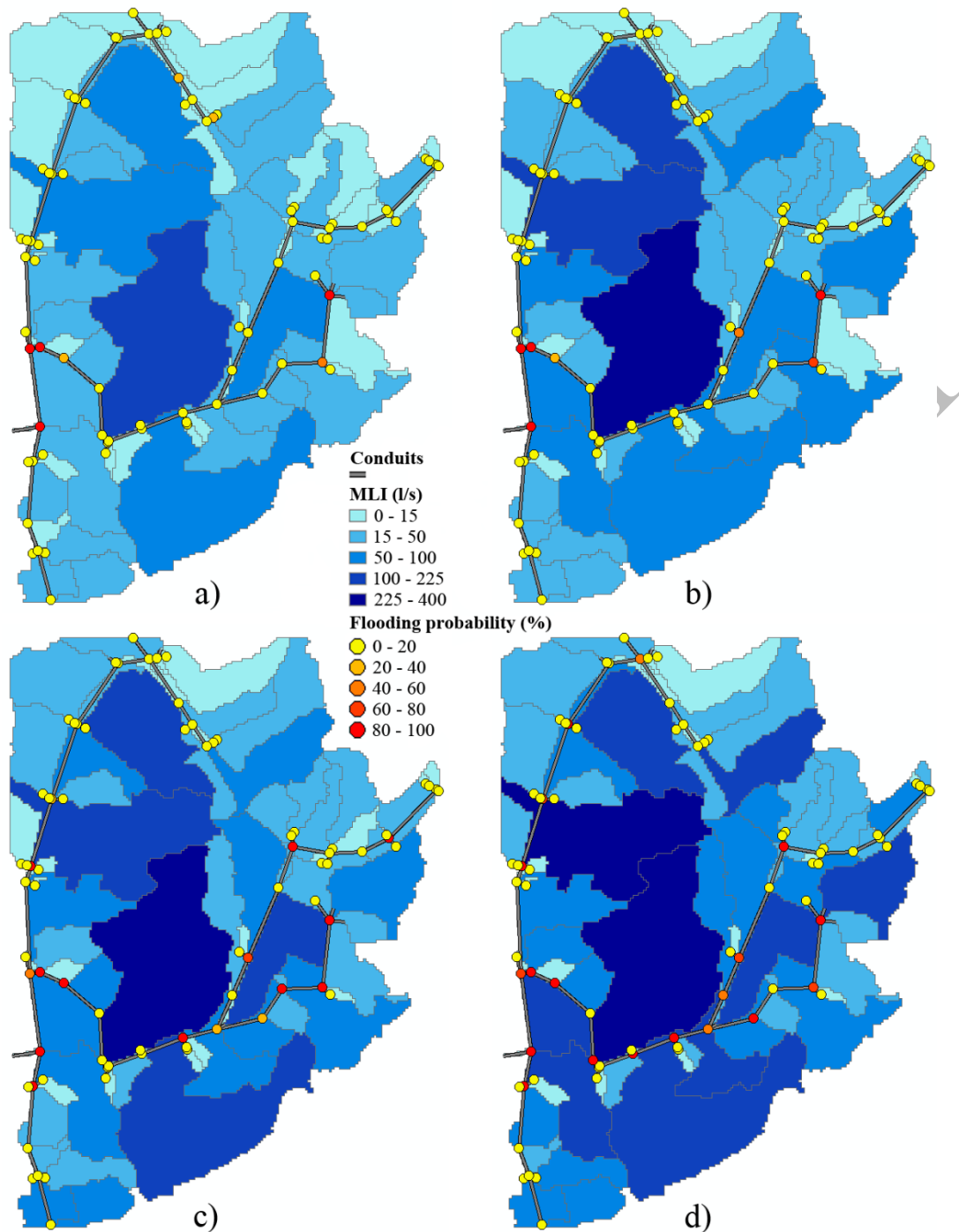
Event	Equation	Adj. Dev. R^2	AIC	H-L
RCP4.5; T = 5 yr.	$y' = -0.49 - 0.26 * x_{1.2} + 0.01 * x_{2.3} + 0.06 * x_{2.4}$	0.83	84.23	0.42
RCP8.5; T = 5 yr.	$y' = -0.17 - 0.26 * x_{1.2} + 0.08 * x_{2.2} + 0.01 * x_{2.3}$	0.81	80.32	0.37
RCP4.5; T = 50 yr.	$y' = -26.41 - 0.13 * x_{1.2} + 0.41 * x_{1.4} + 6.23 * x_{2.1} + 0.11 * x_{2.2} + 18.39 * x_{2.5}$	0.79	88.41	0.07
RCP8.5; T = 25 yr.	$y' = -27.83 + 11.09 * x_{1.1} + 9.79 * x_{2.1} + 22.13 * x_{2.5} - 0.29 * x_{2.9}$	0.74	106.36	0.19

426

427 The quality of these models was ensured by the high and low values of adjusted
428 deviance R^2 and Akaike Information Criterion (AIC) reached, which guaranteed the suitability
429 of the predictors included in the equations presented in Table 6 to predict flooding probabilities.
430 Moreover, the results of the Hosmer-Lemeshow (H-L) test for the four MBLR models built
431 yielded p-values above the significance level ($\alpha = 0.05$) in all cases, which further validated
432 their goodness-of-fit. Consequently, the inclusion of the ratio of MTI to MLI as the frequency
433 in MBLR demonstrated to be a key factor to enhance the fit between predicted and simulated
434 probabilities of flooding.

435 The values obtained for MLI and flooding probability were imported to GIS and
436 mapped as depicted in Fig. 7. MLI was represented according to the subcatchments based on
437 their peak runoff rates, in order to determine their degree of contribution to the nodes to which
438 they flowed, whilst flooding probability was illustrated through the nodes forming the sewer
439 network under study. Since the Climate Change events used to test the methodology provided
440 the ranges of values for which drainage systems will have to be designed in the future to prevent
441 the occurrence of floods in the catchment, this map provided the information required to plan
442 water management strategies to take priority action in vulnerable areas.

443



444

445 **Fig. 7.** Maximum Lateral Inflow (MLI, l/s) and Flooding Probability (%) in the subcatchments and nodes in the
 446 study area

447

448 The results represented in Fig. 7 for short return periods (RCP4.5; T = 5 yr. and RCP8.5;
 449 T = 5 yr.) indicated that oversizing the existing sewer network would not result in a relevant
 450 improvement of the drainage capacity of the catchment, since aspects like the depth and
 451 diameter of its nodes and conduits were not significantly correlated to its flooding susceptibility

452 from a statistical point of view (Table 6). On the contrary, the implementation of Sustainable
453 Drainage Systems (SuDS), also known as BMPs, Low Impact Development (LID) or Water
454 Sensitive Urban Design (WSUD), in those areas with higher values of MLI might decrease the
455 degree of imperviousness of these subcatchments and therefore reduce the amount of lateral
456 inflow received by the nodes of the sewer network too. Di Matteo et al. (2017) and Meerow
457 and Newell (2017) highlighted the importance of the spatial distribution of SuDS to improve
458 urban water-related decision-making processes, in order to maximize their impact by locating
459 them at those sites which most contribute to produce flooding, as illustrated in Fig. 7. In fact,
460 the results presented in Jato-Espino et al. (2016b) demonstrated that the installation of
461 Permeable Pavement Systems at the critical areas shown in Fig. 7 prevented the occurrence of
462 floods in the study catchment when simulating the rainfall scenarios from which these
463 phenomena started to occur in the catchment.

464 Although the common return periods used to design urban drainage systems range from
465 2 to 10 years under the assumption of stationarity (Jato-Espino et al. 2016b), Climate Change
466 is expected to accelerate the water cycle in Finland, producing earlier peak flows and increased
467 discharges (Korhonen and Kuusisto 2010). Therefore, exploring the potential consequences
468 derived from storms associated with longer return periods (RCP4.5; T = 50 yr. and RCP8.5; T
469 = 25 yr.) must be a first concern too. According to Table 6, these scenarios would require taking
470 integrated solutions based on extending the capacity of the existing drainage network through
471 larger diameters and invert elevations and smoother slopes, whilst implementing alternative
472 measures to complement its efficiency, such as installing SuDS and/or including new nodes to
473 divide existing subcatchments into smaller areas and reduce high inflow rates in some nodes.
474 The maps illustrated in Fig. 7 can be of great help for focusing on critical areas and optimize
475 the planning and management of resources to prevent floods.

476

477 **Conclusions**

478

479 This paper proposed and validated a methodology based on Multiple Regression Analysis
480 (MRA) for assessing flood risk in urban catchments. Multiple Linear Regression (MLR) was
481 applied to select catchment and sewer networks parameters proving to be influential in the
482 occurrence of runoff peaks in urban areas, whilst Multiple Non-Linear Regression (MNL
483 and Multiple Binary Logistic Regression (MBLR) models were built to make predictions of
484 Maximum Lateral Inflow (MLI) and Maximum Total Inflow (MTI) in urban catchments and
485 determine the probability of flooding across them, respectively.

486 The excellent values reached in the MNLR models for the predicted coefficient of
487 determination proved that the combination of catchment and sewer network parameters,
488 especially subcatchment area and cumulative length of preceding conduits, can provide
489 accurate estimates of the maximum peak flow rates in subcatchments and nodes. The
490 subsequent use of MBLR provided high-accuracy prediction models to determine the flooding
491 probability associated with the nodes of sewer-catchments under different extreme rainfall
492 scenarios produced by Climate Change. The results proved that the implementation of
493 Sustainable Drainage Systems (SuDS) might be enough to mitigate floods for the return periods
494 commonly used for urban designs, whilst integrated approaches combining both conventional
495 and alternative water management measures would be required to deal with more extreme
496 scenarios. The fact that these outcomes were based on easy to acquire and/or produce
497 parameters and their relationships were solid in both physical and statistical terms enabled the
498 extrapolation and generalization of the proposed approach to other case studies, since the
499 interpretation and application of MRA is simple and compatible with Geographic Information
500 Systems (GIS).

501 This methodology is presented as an accessible framework to support the adoption of
502 measures by administrative entities for facilitating their drainage management planning actions
503 and maximizing their impact through their implementation at strategic sites in terms of flood
504 susceptibility. Although the reliability of the results to which it led is not compromised by the
505 location of the study area, further research should consider the application of this methodology
506 to other urban catchments with larger areas, different climate conditions and more complex
507 drainage systems, in order to regionalize the development of prediction models according to
508 the degree of similarity of distinct zones worldwide. The other main future line of action to
509 continue this research should consist of exploring the automation of the proposed methodology
510 through easy-to-use interfaces and/or support tools, so that potential decision-makers and water
511 resources planners without expertise in the statistical techniques considered might apply them
512 by merely providing a series of basic weather and physical inputs.

513

514 **Acknowledgments**

515

516 This paper was possible thanks to the research projects SUPRIS-SUReS (Ref. BIA2015-65240-
517 C2-1-R MINECO/FEDER, UE) and SUPRIS-SUPeI (Ref. BIA2015-65240-C2-2-R
518 MINECO/FEDER, UE), financed by the Spanish Ministry of Economy and Competitiveness
519 with funds from the State General Budget (PGE) and the European Regional Development
520 Fund (ERDF). The authors wish to express their gratitude to all the entities that provided the
521 data necessary to develop this research: Helsinki Region Environmental Services Authority
522 HSY, Map Service of Espoo, National Land Survey of Finland, Geological Survey of Finland,
523 EURO-CORDEX and European Climate Assessment & Dataset.

524

525 **References**

526

527 Aiken, L. S., West, S. G., and Pitts, S. C. (2003). "Multiple Linear Regression." *Handbook of*
528 *Psychology*, John Wiley & Sons, Inc., New York (U.S.).

529 Akaike, H. (1973). "Information theory as an extension of the maximum likelihood principle."
530 *Second International Symposium on Information Theory*, B. N. Petrov, and F. Csaki,
531 eds., Akademiai Kiado, Budapest (Hungary), 267-281.

532 Ashley, R., Garvin, S., Pasche, E., Vassilopoulos, A., and Zevenbergen, C. (2007). *Advances*
533 *in Urban Flood Management*. CRC Press, London (U.K.).

534 Barco, J., Wong, K. M., and Stenstrom, M. K. (2008). "Automatic calibration of the U.S. EPA
535 SWMM model for a large urban catchment." *Journal of Hydraulic Engineering*, 134(4),
536 466-474.

537 Beck, N. G., Conley, G., Kanner, L., and Mathias, M. (2017). "An urban runoff model designed
538 to inform stormwater management decisions." *Journal of Environmental Management*,
539 193 257-269.

540 Di Matteo, M., Dandy, G. C., and Maier, H. R. (2017). "Multiobjective Optimization of
541 Distributed Stormwater Harvesting Systems." *Journal of Water Resources Planning*
542 *and Management*, Just Released.

543 Dongquan, Z., Jining, C., Haozheng, W., Qingyuan, T., Shangbing, C., and Zheng, S. (2009).
544 "GIS-based urban rainfall-runoff modeling using an automatic catchment-discretization
545 approach: A case study in Macau." *Environmental Earth Sciences*, 59(2), 465-472.

546 Elliott, A. H., and Trowsdale, S. A. (2007). "A review of models for low impact urban
547 stormwater drainage." *Environmental Modelling and Software*, 22(3), 394-405.

548 Eshtawi, T., Evers, M., Tischbein, B., and Diekkrüger, B. (2016). "Integrated hydrologic
549 modeling as a key for sustainable urban water resources planning." *Water Research*,
550 101 411-428.

551 Fisher, R. A. (1925). *Statistical Methods for Research Workers*. Cosmo Publications,
552 Edinburgh (Scotland).

553 Guan, M., Sillanpää, N., and Koivusalo, H. (2015). "Modelling and assessment of hydrological
554 changes in a developing urban catchment." *Hydrological Processes*, 29(13), 2880-
555 2894.

556 Hammond, M. J., Chen, A. S., Djordjevic, S., Butler, D., and Mark, O. (2015). "Urban flood
557 impact assessment: A state-of-the-art review." *Urban Water Journal*, 12(1), 14-29.

558 Hanington, P., To, Q. T., Van, P. D. T., Doan, N. A. V., and Kiem, A. S. (2017). "A
559 hydrological model for interprovincial water resource planning and management: A
560 case study in the Long Xuyen Quadrangle, Mekong Delta, Vietnam." *Journal of*
561 *Hydrology*, 547 1-9.

562 Hegger, D. L. T., Driessen, P. P. J., Wiering, M., Van Rijswijk, H. F. M. W., Kundzewicz, Z.
563 W., Matczak, P., Crabbé, A., Raadgever, G. T., Bakker, M. H. N., Priest, S. J., Larrue,
564 C., and Ek, K. (2016). "Toward more flood resilience: Is a diversification of flood risk
565 management strategies the way forward?" *Ecology and Society*, 21(4), 52.

566 Hoornweg, D., Freire, M., Lee, M. J., Perinaz Bhada-Tata, P., and Yuen, B. (2011). *Cities and*
567 *Climate Change: Responding to an Urgent Agenda*. World Bank Publications,
568 Washington, D.C. (U.S.).

569 Hosmer, D. W., and Lemeshow, S. (2000). *Applied Logistic Regression*. John Wiley & Sons,
570 New York (U.S.).

571 Huntington, T. G. (2006). "Evidence for intensification of the global water cycle: Review and
572 synthesis." *Journal of Hydrology*, 319(1-4), 83-95.

573 Huong, H. T. L., and Pathirana, A. (2013). "Urbanization and climate change impacts on future
574 urban flooding in Can Tho city, Vietnam." *Hydrology and Earth System Sciences*,
575 17(1), 379-394.

576 Jato-Espino, D., Charlesworth, S. M., Bayon, J. R., and Warwick, F. (2016a). "Rainfall–Runoff
577 Simulations to Assess the Potential of SuDS for Mitigating Flooding in Highly
578 Urbanized Catchments." *International Journal of Environmental Research and Public
579 Health*, 13(1), 149.

580 Jato-Espino, D., Sillanpää, N., Charlesworth, S. M., and Andrés-Doménech, I. (2017). "A
581 simulation-optimization methodology to model urban catchments under non-stationary
582 extreme rainfall events." *Environmental Modelling and Software*, In Press.

583 Jato-Espino, D., Sillanpää, N., Charlesworth, S. M., and Andrés-Doménech, I. (2016b).
584 "Coupling GIS with Stormwater Modelling for the Location Prioritization and
585 Hydrological Simulation of Permeable Pavements in Urban Catchments." *Water
586 (Switzerland)*, 8(10), 451.

587 Knebl, M. R., Yang, Z. -, Hutchison, K., and Maidment, D. R. (2005). "Regional scale flood
588 modeling using NEXRAD rainfall, GIS, and HEC-HMS/ RAS: A case study for the
589 San Antonio River Basin Summer 2002 storm event." *Journal of Environmental
590 Management*, 75(4 SPEC. ISS.), 325-336.

591 Korhonen, J., and Kuusisto, E. (2010). "Long-term changes in the discharge regime in Finland."
592 *Hydrology Research*, 41(3-4), 253-268.

593 Meerow, S., and Newell, J. P. (2017). "Spatial planning for multifunctional green
594 infrastructure: Growing resilience in Detroit." *Landscape and Urban Planning*, 159 62-
595 75.

596 Minitab Inc. (2016). "Minitab® 17." <https://www.minitab.com/en-us/products/minitab/> (11/09,
597 2016).

598 Moss, R., Babiker, M., Brinkman, S., Calvo, E., Carter, T., Edmonds, J., Elgizouli, I., Emori,
599 S., Erda, L., Hibbard, K., Jones, R., Kainuma, M., Kelleher, J., Lamarque, J. F.,
600 Manning, M., Matthews, B., Meehl, J., Meyer, L., Mitchell, J., Nakicenovic, N.,
601 O'Neill, B., Pichs, R., Riahi, K., Rose, S., Runci, P., Stouffer, R., van Vuuren, D.,
602 Weyant, J., Wilbanks, T., van Ypersele, J. P., and Zurek, M. (2008). "III.
603 "Representative Concentration Pathways"." *Towards New Scenarios for Analysis of*
604 *Emissions, Climate Change, Impacts, and Response Strategies*, Intergovernmental
605 Panel on Climate Change (IPCC), Geneva (Switzerland), 5-25.

606 Osbourne, J. W., and Waters, E. (2002). "Four Assumptions of Multiple Regression That
607 Researchers Should Always Test." *Practical Assessment, Research & Evaluation*, 8 1-
608 7.

609 Sillanpää, N., and Koivusalo, H. (2015). "Impacts of urban development on runoff event
610 characteristics and unit hydrographs across warm and cold seasons in high latitudes."
611 *Journal of Hydrology*, 521 328-340.

612 Smith, K., and Ward, R. (1998). *Floods: Physical Processes and Human Impacts*. John Wiley
613 & Sons, Chichester (U.K.).

614 Tingsanchali, T. (2012). "Urban flood disaster management." *3rd International Science, Social*
615 *Science, Engineering and Energy Conference 2011, I-SEEC 2011*, 25-37.

616 USEPA. (2016). "Storm Water Management Model (SWMM) - Version 5.1.011 with Low
617 Impact Development (LID) Controls." [https://www.epa.gov/water-research/storm-](https://www.epa.gov/water-research/storm-water-management-model-swmm)
618 [water-management-model-swmm](https://www.epa.gov/water-research/storm-water-management-model-swmm) (11/09, 2016).

619 Yao, L., Chen, L., and Wei, W. (2017). "Exploring the linkage between urban flood risk and
620 spatial patterns in small urbanized catchments of Beijing, China." *International Journal*
621 *of Environmental Research and Public Health*, 14(3).